Coaggregation, Cointernalization, and Codesensitization of Adenosine A$_{2A}$ Receptors and Dopamine D$_2$ Receptors*

**Joëlle Hillion‡§¶, Meritxell Canals‡§, Maria Torvinen‡, Vicent Casadó‖, Rizaldy Scott‡,
Anton Terasmaa‡, Anita Hansson‡, Stanley Watson**, Mark E. Olah‡‡, Josefa Mallol‖,
Enric I. Canela‖, Michele Zoli§§, Luigi F. Agnati§§, Carlos F. Ibáñez‡, Carme Lluis‖,
Rafael Franco‖, Sergi Ferré‡ ¶¶, and Kjell Fuxe‡**

*From the ‡Department of Neuroscience, Karolinska Institute, 17177 Stockholm, Sweden, the ‖Department of Biochemistry
and Molecular Biology, University of Barcelona, 08028 Barcelona, Spain, the **Mental Health Institute, University of
Michigan, Ann Arbor, Michigan 48109, the ‡‡Department of Medicine, Duke University Medical Center, Durham, North
Carolina 27710, the §§Department of Biomedical Sciences, University of Modena, 41100 Modena, Italy, and the
¶¶National Institute on Drug Abuse, Baltimore, Maryland 21224*

Antagonistic and reciprocal interactions are known to exist between adenosine and dopamine receptors in the striatum. In the present study, double immunofluorescence experiments with confocal laser microscopy showed a high degree of colocalization of adenosine A$_{2A}$ receptors (A$_{2A}$R) and dopamine D$_2$ receptors (D$_2$R) in cell membranes of SH-SY5Y human neuroblastoma cells stably transfected with human D$_2$R and in cultured striatal cells. A$_{2A}$R/D$_2$R heteromeric complexes were demonstrated in coimmunoprecipitation experiments in membrane preparations from D$_2$R-transfected SH-SY5Y cells and from mouse fibroblast Ltk$^-$ cells stably transfected with human D$_2$R (long form) and transiently cotransfected with the A$_{2A}$R double-tagged with hemagglutinin. Long term exposure to A$_{2A}$R and D$_2$R agonists in D$_2$R-cotransfected SH-SY5Y cells resulted in coaggregation, cointernalization and codesensitization of A$_{2A}$R and D$_2$R. These results give a molecular basis for adenosine-dopamine antagonism at the membrane level and have implications for treatment of Parkinson's disease and schizophrenia, in which D$_2$R are involved.

Adenosine and dopamine signaling exert opposite effects in the basal ganglia, a brain region involved in sensory-motor integration. Thus, adenosine agonists induce motor depression and adenosine antagonists, such as caffeine, produce motor activation (1). These opposite effects result from specific antagonistic interactions between subtypes of adenosine and dopamine receptors in the striatum, the main input structure of the basal ganglia. In fact, striatal dopamine receptors and, to some extent, adenosine receptors are segregated in the two main populations of γ-aminobutyric acid (GABA) efferent neurons. Striopallidal neurons express dopamine receptors predominantly of the D$_2$ subtype (D$_2$R)[1] and the highest density of adenosine A$_{2A}$ receptors (A$_{2A}$R) in the brain (2, 3). In the rat, the strionigro-strioentopeduncular neurons contain dopamine receptors predominantly of the D$_1$ subtype (D$_1$R) and express exclusively adenosine receptors of the A$_1$ subtype (A$_1$R) (2–4). Experimental evidence supports the existence of antagonistic A$_{2A}$R/D$_2$R and A$_1$R/D$_1$R interactions, respectively, in the GABA striopallidal and strionigro-strioentopeduncular neurons (1, 5). Taken together, these data suggested proximity between receptors, which could allow them to form heteromeric complexes (directly or indirectly by means of adaptor proteins). In fact, A$_1$R and D$_1$R were found to form heteromeric complexes (6). Although antagonistic A$_{2A}$R/D$_2$R interactions have been reported to play an important role in basal ganglia function, it is still not known whether the formation of heteromeric A$_{2A}$R/D$_2$R complexes is also involved. In the present work, the existence of selective intramembrane interactions between A$_{2A}$R and D$_2$R in neuronal cells is demonstrated, including formation of heteromeric A$_{2A}$R/D$_2$R complexes and their potential involvement in cross-desensitization mechanisms via agonist-induced coaggregation and cointernalization of A$_{2A}$R and D$_2$R. These results have clinical implications for Parkinson's disease and other basal ganglia disorders where dopamine D$_2$R are the target for therapy (1, 5).

EXPERIMENTAL PROCEDURES

Cell Cultures—Maintenance of SH-SY5Y cells (parental and D$_2$R-transfected cells) as well as the pharmacological characterization and maintenance of D$_2$R- and D$_1$R-transfected mouse fibroblast Ltk$^-$ cells are described in detail elsewhere (7–9). For primary cultures, striata were removed from 16-day-old Sprague-Dawley rat embryos (B&K Universal) in Ca^{2+}/Mg^{2+}-free PBS supplemented with 20 units/ml penicillin and 20 μg/ml streptomycin (Invitrogen). The tissue fragments were pooled and mechanically dissociated in SFM Neurobasal serum-free medium (Invitrogen), supplemented with B27 (Invitrogen), glutamine (2 mM; Invitrogen), penicillin/streptomycin (20 units/ml/20 μg/ml; Invitrogen), and β-mercaptoethanol (25 μM) (Invitrogen). Cells were collected by centrifugation at 100 × g for 5 min and resuspended in fresh medium. The resulting single-cell suspension was seeded on 24-well plates coated with gelatin (Sigma) and poly-L-lysine (Sigma), and cells were grown at 37 °C in saturation humidity with 5% CO$_2$.

Immunolabeling Experiments—Neuroblastoma cells were grown on glass coverslips coated with poly-L-lysine (Sigma) and exposed to vari-

[1] The abbreviations used are: D$_2$R, dopamine D$_2$ receptor; A$_{2A}$R, adenosine A$_{2A}$ receptor; HA, hemagglutinin; ANOVA, analysis of variance; PBS, phosphate-buffered saline; FITC, fluorescein isothiocyanate; IR, immunoreactive; GI, Gini's index; DOPA, 3,4-dihydroxyphenylalanine.
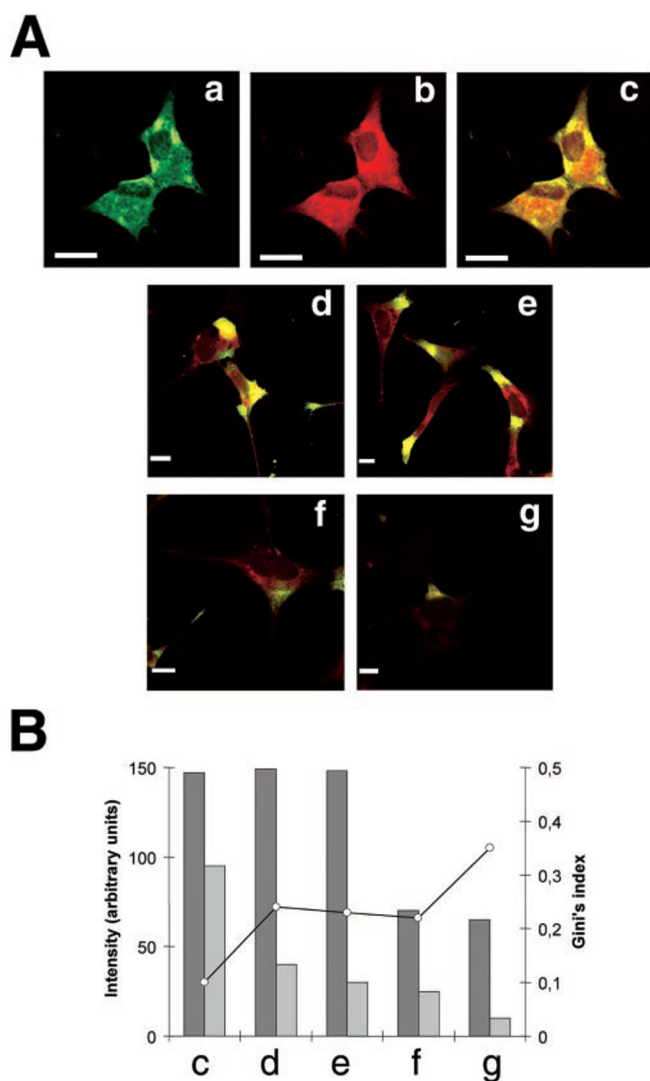
FIG. 1. *A*, double immunofluorescence staining and confocal images of SH-SY5Y neuroblastoma cells stably transfected with the cDNA encoding for human D$_2$R (long form). Cells were processed for immunostaining using fluorescein (*green*)-conjugated rabbit anti-A$_{2A}$R antibodies and rhodamine (*red*)-conjugated rabbit anti-D$_2$R antibodies and analyzed by confocal microscopy. Superimposition of images (*panels c–h*) reveals the colocalization of A$_{2A}$R and D$_2$R in *yellow*. *Panels a–c* show A$_{2A}$R immunoreactivity (*a*), D$_2$R immunoreactivity (*b*), and A$_{2A}$R/D$_2$R colocalization (*c*) in nontreated cells (no agonist preincubation). *Panels d–g* show the effects of 3 h of treatment at 37 °C with CGS-21680 (100 nM) alone (*d*), quinpirole (10 μM) alone (*e*), CGS-21680 (100 nM) and quinpirole (10 μM) (*f*), or CGS-21680 (200 nM) and quinpirole (50 μM) (*g*). Cells were processed for immunostaining after agonist preincubation. Representative images from four independent experiments/treatment are shown; *scale bars*, 10 μm. *B*, semiquantitation of images from *panels c–g* in *A*. The area (*light gray*) where diffuse IR (no or few coaggregates) and the area (*dark gray*) where several coaggregates could be detected were interactively selected. The median intensity values (*left y* axis) for these two types of areas, obtained in the four experimental conditions mentioned above (*c–g*), are given. The Gini's indexes (*right y* axis) for the four experimental conditions (*c–g*) are given. It should be noticed that the Gini's index is low (rather even distribution of the IR intensity among pixels) for nontreated cells (*c*), whereas the Gini's index is high (rather uneven distribution of the IR intensity among pixels) for co-treatment with CGS-21680 (200 nM) plus quinpirole (50 μM) (*g*).

ous amounts of CGS21680 (RBI) and/or quinpirole (RBI) in serum-free medium for 3 h at 37 °C. They were then rinsed with PBS, fixed in 4% paraformaldehyde and 0.06 M sucrose for 15 min, and washed with PBS containing 20 mM glycine. Cells were subsequently treated with PBS, containing 20 mM glycine, and 1% bovine serum albumin for 30 min at room temperature. Double immunostaining was performed with fluo-
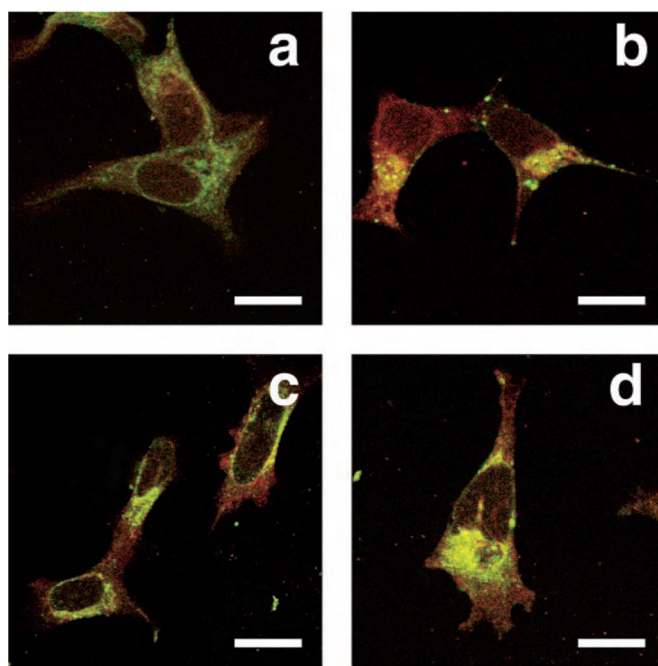
FIG. 2. **Agonist-induced internalization of A$_{2A}$R and D$_2$R in SH-SY5Y neuroblastoma cells stably transfected with the cDNA encoding for human D$_2$R (long form).** Cells were processed for immunostaining using fluorescein (*green*)-conjugated rabbit anti-A$_{2A}$R antibodies and rhodamine (*red*)-conjugated rabbit anti-D$_2$R antibodies and analyzed by confocal microscopy. Superimposition of images reveals the colocalization of A$_{2A}$R and D$_2$R (*yellow*). Cells were first incubated with anti-A$_{2A}$R and anti-D$_2$R antibodies for 2 h at 4 °C in the presence (*b–d*) or absence (*a*) of the agonists. The cells were then placed at 37 °C for 3 h allowing ligand-induced internalization of previously labeled receptors. *Panel a* shows the weak diffuse immunoreactivity of nonpretreated control cells (compare with Fig. 1, *panels c*). *Panels b–d* show the effects of 3 h of treatment at 37 °C with CGS-21680 (200 nM) alone (*b*), quinpirole (50 μM) alone (*c*), or CGS-21680 (200 nM) and quinpirole (50 μM) (*d*). Representative images from four independent experiments/treatment are shown; *scale bars*, 10 μm.

rescein-conjugated anti-A$_{2A}$R antibodies (VC21-FITC, 40 μg/ml) (10) and rhodamine-conjugated anti-D$_2$R antibodies (D2-246-316, 30 μg/ml) (11) for 1 h at 37 °C. Antipeptide antisera against A$_{2A}$R were raised in New Zealand White rabbits and characterized as described elsewhere (12). The specific peptide corresponds to the second extracellular loop of the receptor. Anti-A$_{2A}$R antibodies (VC21) were purified by affinity chromatography using the specific peptide coupled to activated thiol-Sepharose 4B. The coverslips were rinsed for 40 min in the same buffer and mounted with medium suitable for immunofluorescence (ICN). Internalization assays were made as reported elsewhere (12) with some modifications. Cells were incubated in serum-free medium (4 °C, 2 h) with VC21-FITC and rhodamine-conjugated D2-246-316 in the absence (control) or presence of 200 nM CGS 21680 and/or 50 μM quinpirole. Cells were washed with the same medium (without ligands in the control experiments), and internalization of labeled receptors was induced by incubation at 37 °C for 3 h. Cells were fixed and processed as described above. Striatal cultures were exposed to various amounts of CGS21680 and/or quinpirole in the same medium for 6 h at 37 °C. They were then rinsed with PBS, fixed with 4% paraformaldehyde containing 2% picric acid for 1 h, and washed with PBS supplemented with 20 mM glycine. Double or single immunostaining was performed with fluorescein-conjugated anti-A$_{2A}$R antibodies and rhodamine-conjugated anti-D$_2$R (D2-246-316) antibodies or fluorescein-conjugated anti-A$_1$R antibodies (PC21-FITC) (13) for 1 h at 37 °C. Microscopic observations were made in Leica TCS 4D (Leica Lasertechnik) confocal scanning laser equipment adapted to an inverted Leitz DMIRBE microscope. Image analysis was performed with a KS 400 image analyzer (Zeiss). After acquisition of the superimposed images (yellow color) of the A$_{2A}$R/D$_2$R IR, the area of the cell nucleus was interactively discarded. Densitometric evaluation was performed on this new image. The median values of the histograms representing the intensity of A$_2$R/D$_2$R IR in areas with coaggregates (interactively encircled) and in areas with no or few aggregates (interactively encircled) were taken as representative val-
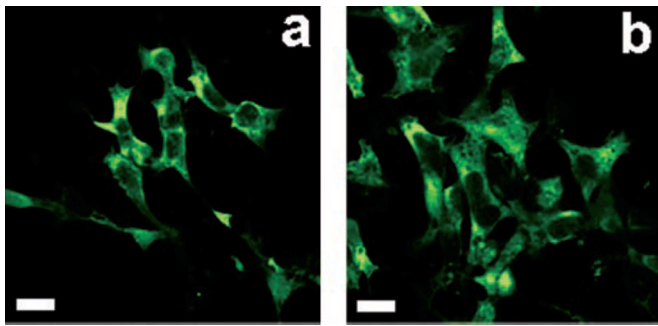
F$_{IG}$. 3. **Immunostaining of parental SH-SY5Y neuroblastoma cells.** Untransfected SH-SY5Y cells were processed for immunostaining using fluorescein (*green*)-conjugated rabbit anti-A$_{2A}$R antibodies after exposure to medium in the absence (*a*) or presence (*b*) of 100 μM quinpirole (3 h, 37 °C). Representative images from three independent experiments are shown; *scale bar*, 10 μm.

ues in their respective areas. A quantitative evaluation of the degree of unevenness of the A$_{2A}$R/D$_2$R receptor codistribution was obtained by calculating the Gini's index (14, 15), which here measures the distribution of the IR intensity, pixel by pixel, in the sampled area. The Gini's index ranges from 0 (even distribution, *i.e.* the IR intensity is equally distributed among pixels) to 1 (maximal concentration, *i.e.* the IR intensity is concentrated in one single pixel) (14).

Coimmunoprecipitation Experiments—SH-SY5Y neuroblastoma cell membranes were obtained by disrupting the cells with a Polytron homogenizer (Kinematica, PTA 20TS rotor, setting 4; Brinkmann) for three 5-s periods in 50 mM Tris-HCl, pH 7.4. Membranes were separated by centrifugation at 105,000 × *g* for 45 min at 4 °C. They were then solubilized in ice-cold lysis buffer (PBS, pH 7.4, Nonidet P-40, 0.5% sodium deoxycholate, 0.1% SDS) for 1 h on ice and then centrifuged at 80,000 × *g* for 90 min. The supernatant was immunoprecipitated as previously described (6) using anti-A$_{2A}$R antibodies (VC21) or an irrelevant IgG covalently coupled to protein A-Sepharose. Immunoprecipitates were resolved by SDS-PAGE, and Western blots were performed with anti-A$_{2A}$R, anti-A$_1$R (PC11), or anti-D$_2$R antibodies (for details, see Ref. 6).

D$_2$R- and D$_1$R transfected mouse fibroblast Ltk$^-$ cells were transiently transfected with A$_{2A}$R cDNA double-tagged with hemagglutinin (HA-A$_{2A}$R-HA) (16) by calcium phosphate precipitation (8, 9). Immunoprecipitation of HA-A$_{2A}$R-HA was performed with anti-HA antibodies (Babco) covalently coupled to protein G-Sepharose. Immunoprecipitation and immunoblotting were done following standard protocols (6). Immunoblots were developed with ECL Western blot detection system.

cAMP Accumulation Experiments—Neuroblastoma or striatal cells were incubated with [^{3}H]adenine (24 Ci/mmol; Amersham Biosciences; 1 μCi/well) for 2 h at 37 °C in serum-free medium. They were subsequently washed with PBS and incubated for 10 min at 37 °C in PBS containing 100 μM phosphodiesterase inhibitor RO-20-1724 (Calbiochem). Various concentrations of forskolin, CGS 21680, and/or quinpirole were then added and the cells placed at 37 °C for an additional 10 min. The incubation solution was then discarded and replaced by ice-cold 0.3 M perchloric acid containing [^{14}C]cAMP (51.3 mCi/mmol; PerkinElmer Life Sciences) as an internal standard. After sonication and centrifugation (8,000 × *g* for 5 min), [^{3}H]cAMP present in the supernatant was identified by sequential chromatography (17). Formation of cAMP was expressed as the percentage of conversion of total [^{3}H]ATP into [^{3}H]cAMP. For statistical analysis, one-way ANOVA (followed by *post hoc* Scheffe's multiple comparison test) and Mann-Whitney's *U* test were used.

RESULTS

Colocalization of A$_{2A}$R and D$_2$R in Nontreated SH-SY5Y Neuroblastoma Cells: Immunolabeling Experiments—A$_{2A}$R/D$_2$R interactions were first studied in a previously characterized human neuroblastoma cell line (SH-SY5Y) stably transfected with human D$_2$R (long form) (about 1100 fmol/mg of protein) (7). This cell line constitutively expresses functional A$_{2A}$R (about 200 fmol/mg of protein), the activation of which decreases the affinity of the transfected D$_2$R for dopamine and counteracts D$_2$R-mediated intracellular [Ca^{2+}]$_i$ response (7). Double immunofluorescence experiments including image

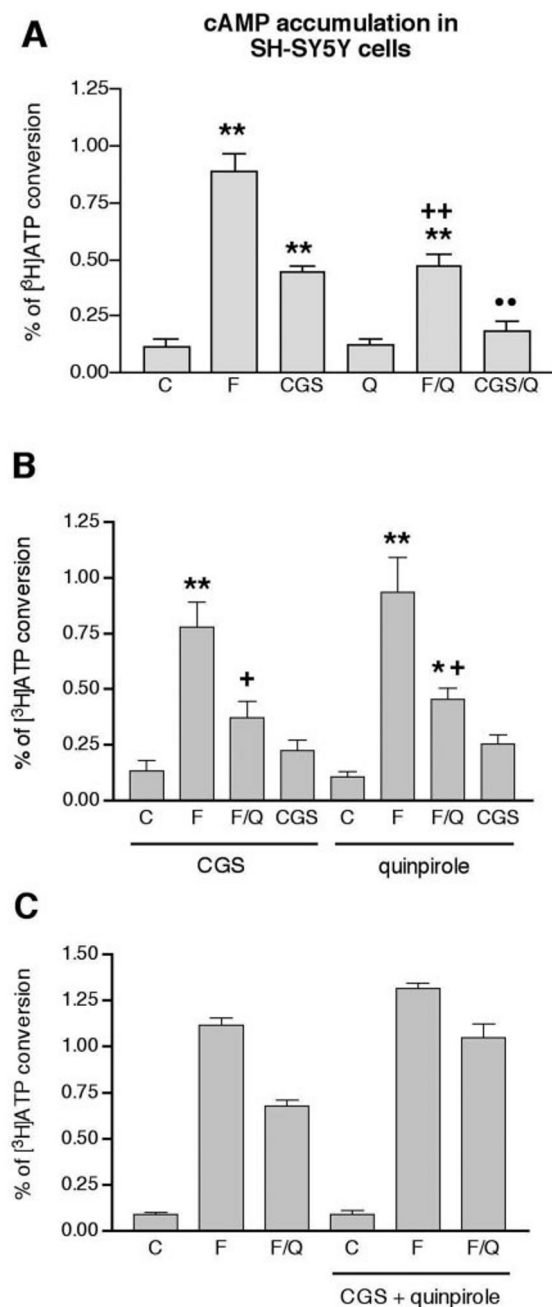F$_{IG}$. 4. **cAMP accumulation experiments in SH-SY5Y neuroblastoma cells stably transfected with D$_2$R (long form).** Results represent means ± S.E. and are expressed as percentage of conversion of total [^{3}H]ATP to [^{3}H]cAMP (*n* = 6–8). *A*, effects of 10 μM forskolin (*F*), 1 μM CGS 21680 (*CGS*), and 1 μM quinpirole (*Q*), alone or in combination, without agonist preincubation. Quinpirole significantly decreased forskolin- and CGS-induced cAMP accumulation. **, *p* < 0.01 compared with control (*C*); ++, *p* < 0.01 compared with forskolin; ··, *p* < 0.01 compared with CGS; one-way ANOVA and *post hoc* Scheffe's multiple comparison test. *B*, effects of 10 μM forskolin (*F*), 1 μM CGS 21680 (*CGS*), and 1 μM quinpirole (*Q*), alone or in combination, after preincubation for 3 h with either 200 nM CGS 21680 or 50 μM quinpirole. Preincubating the cells with either agonist counteracted CGS 21680-induced cAMP accumulation. ** and *, *p* < 0.01 and *p* < 0.05, respectively, compared with control (*C*); +, *p* < 0.05 compared with forskolin; one-way ANOVA and *post hoc* Scheffe's multiple comparison test. *C*, effects of 10 μM forskolin in the absence (*F*) and presence of 1 μM quinpirole (*F/Q*) with and without preincubation for 3 h with 200 nM CGS 21680 and 50 μM quinpirole. The counteractive effect of quinpirole on forskolin-induced cAMP accumulation was significantly lower after simultaneous preincubation with A$_{2A}$R and D$_2$R agonists (17.1%/11.4%, in median/interquartile range; *n* = 7) than without preincubation (40.7%/5.8%, in median/interquartile range; *n* = 7) (*p* < 0.01; Mann-Whitney *U* test).

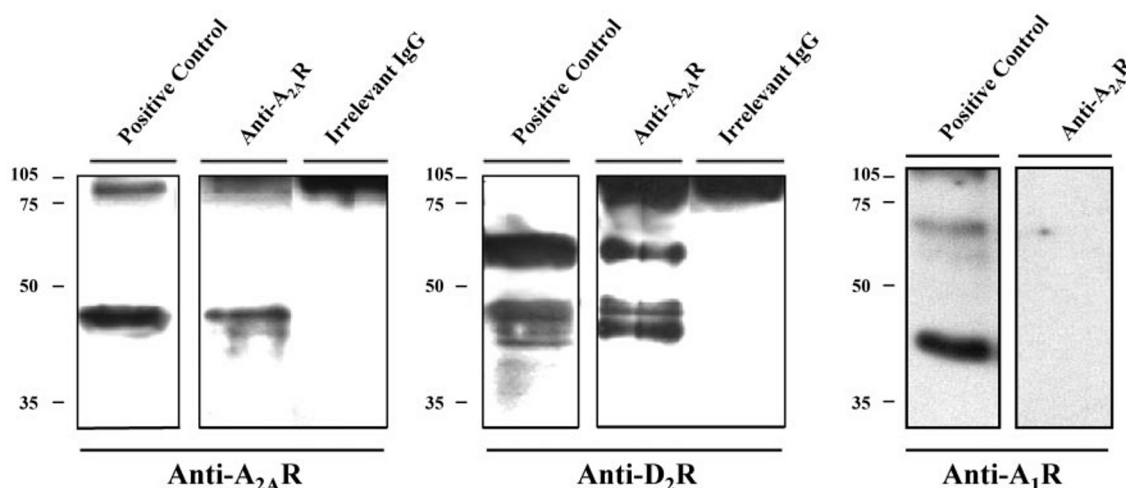*Adenosine A$_{2A}$ Receptor/Dopamine D$_2$ Receptor Interactions*

FIG. 5. **Coimmunoprecipitation of A$_{2A}$R and D$_2$R from membrane preparations of SH-SY5Y neuroblastoma cells stably transfected with D$_2$R (long form).** Immunoprecipitation with anti-A$_{2A}$R antibodies was followed by Western blotting with antibodies against A$_{2A}$R (*left*), against D$_2$R (*middle*), or against A$_1$R (*right*). For positive control an aliquot of cell membrane extracts was used.

analysis were performed in nonpermeabilized cells, using fluorescein-conjugated anti-A$_{2A}$R antibodies (*green color*) and rhodamine-conjugated anti-D$_2$R antibodies (*red color*). As seen in Fig. 1*A* (*panels a* and *b*), there is a clear spatial predominance of D$_2$R *versus* A$_{2A}$R immunoreactivity, which is in agreement with the higher D$_2$R density found in previous binding experiments (7). Confocal analysis revealed substantial colocalization of both receptors at the membrane level (*yellow color* in Fig. 1*A*, *panel c*), which indicates that in the absence of exogenous agonists the lateral distance between the two receptor proteins is less than 0.1 μm. A semi-quantitative analysis of the distribution of the *yellow* was done by evaluating the intensity of the color (which directly reflects the amount of coexisting receptors) and calculating the Gini's index or GI (a measure of unevenness, which evaluates the proportion of coaggregates in the sampled area). These calculations were completed on the whole cell body membrane, as well as on the areas of the cell body membrane containing coaggregates and on the parts with few or no coaggregates (Fig. 1*B*). In nontreated cells (Fig. 1*A*, *panel c*), high amounts of coexisting receptors were found both in the cell body membrane with coaggregates and in the cell body membrane displaying a more diffuse distribution of A$_{2A}$R/D$_2$R IR. The GI value of these cells was 0.10, indicating a rather even distribution of the colocated A$_{2A}$R/D$_2$R IR and few coaggregates of the two receptors (Fig. 1*B*).

Coaggregation of A$_{2A}$R and D$_2$R in CGS 21680- or Quinpirole-treated SH-SY5Y Cells: Immunolabeling Experiments—Substantial modifications of A$_{2A}$R and D$_2$R distribution were obtained when the cells were treated with the A$_{2A}$R agonist CGS 21680 or the D$_2$R agonist quinpirole. Hence, 3 h of treatment with either CGS 21680 (100 nM, Fig. 1*A*, *panel d*) or quinpirole (10 μM, Fig. 1*A*, *panel e*) induced an aggregation of both A$_{2A}$R and D$_2$R. Similar effects were also observed with shorter incubation times at higher agonist concentrations (data not shown). Thus, 3 h of incubation at these concentrations give a maximal effect. The computer-assisted analysis of the confocal images showed an increase in unevenness of the yellow distribution (GI for the entire cell body membrane was 0.23 for CGS 21680- and 0.20 for quinpirole-treated cells). Furthermore, the yellow intensity value was still high for the cell body membrane with A$_{2A}$R/D$_2$R coaggregates but very low for the cell body membrane with diffusely distributed A$_{2A}$R/D$_2$R IR (Fig. 1*B*). Altogether, this analysis indicates the presence on the cell body membrane of an increased proportion of A$_{2A}$R/D$_2$R coaggregates.

Cointernalization of A$_{2A}$R and D$_2$R in CGS 21680- or Quinpirole-treated SH-SY5Y Cells: Immunolabeling Experiments—Cotreatment with CGS 21680 (100 nM) and quinpirole (10 μM) markedly decreased the yellow intensity values of the cell body membrane associated with coaggregates and diffusely distributed A$_{2A}$R/D$_2$R IR as compared with untreated cells (Fig. 1, *A (panel f)* and *B*). This indicates that cotreatment with CGS 21680 (100 nM) and quinpirole (10 μM) induces coaggregation followed by cointernalization of A$_{2A}$R and D$_2$R. A stronger reduction in D$_2$R IR (*red*) was, however, obtained with higher concentrations of quinpirole (50 μM) and CGS 21680 (200 nM) (Fig. 1*A*, *panel g*). At these concentrations of the agonists, the Gini's index was high (0.30) reflecting an uneven distribution of A$_{2A}$R/D$_2$R IR. In addition, the values for the yellow intensity in the cell body membrane with A$_{2A}$R/D$_2$R coaggregates and the cell body membrane with diffusely distributed A$_{2A}$R/D$_2$R IR were, respectively, low and very low (Fig. 1*B*). This suggests that a cotreatment of the cells with high doses of the agonists potentiates both coaggregation and cointernalization of A$_{2A}$R and D$_2$R. Ligand-induced cointernalization was confirmed in experiments where cells were first labeled with anti-A$_{2A}$R and anti-D$_2$R antibodies for 2 h at 4 °C in the absence (Fig. 2, *panel a*) or in the presence of CGS21680 (200 nM) and/or quinpirole (50 μM) (Fig. 2, *panels b–d*). Subsequently, the ligand-induced internalization of labeled receptors was allowed to occur by incubating the cells for 3 h at 37 °C. Confocal analysis revealed colocalized A$_{2A}$R/D$_2$R aggregates inside the cell after pretreatment with either CGS 21680 (200 nM) or quinpirole (50 μM) (Fig. 2, *panels b* and *c*), which became more pronounced after pretreatment with both compounds (Fig. 2, *panel d*).

Absence of Quinpirole-induced Aggregation of A$_{2A}$R in Parental SH-SY5Y Cells: Immunolabeling Experiments—The involvement of D$_2$R in quinpirole-mediated effects was assessed using parental neuroblastoma SH-SY5Y cells, which express very low levels of D$_2$R (7). Hence, quinpirole at 100 μM for 3 h did not induce any modification of A$_{2A}$R immunolabeling pattern (Fig. 3).

Codesensitization of A$_{2A}$R and D$_2$R in CGS 21680- and Quinpirole-treated SH-SY5Y Cells: cAMP Accumulation Experiments—Under basal conditions 1 μM CGS 21680 significantly increased cAMP accumulation in SH-SY5Y neuroblastoma cells (Fig. 4*A*). Quinpirole (1 μM) did not modify cAMP levels but significantly counteracted both forskolin (10 μM)-induced and CGS 21680-induced increases in cAMP accumulation (Fig. 4*A*). These results confirm the existence of functional and in-
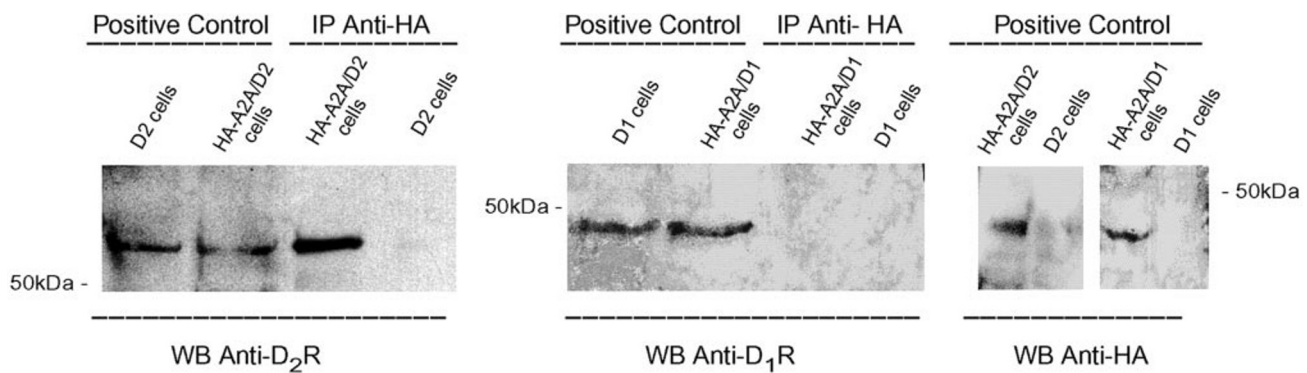
FIG. 6. **Coimmunoprecipitation of HA-A$_{2A}$R-HA and D$_2$R from membrane preparations of mouse Ltk$^-$ fibroblasts.** Ltk$^-$ fibroblasts stably transfected with either human dopamine D$_2$R (long form) or human dopamine D$_1$R were transiently transfected with either double-tagged HA-A$_{2A}$R-HA (HA-A$_{2A}$R-HA/D$_2$R and HA-A$_{2A}$R-HA/D$_1$R cells) or an irrelevant plasmid (D$_2$R and D$_1$R cells). An aliquot of cell membrane extracts was used as a positive control. *WB*, Western blot; *IP*, immunoprecipitation.

teracting A$_{2A}$R and D$_2$R in D$_2$R-transfected neuroblastoma cells (7). After 3 h of incubation with either 200 nM CGS 21680 or 50 μM quinpirole (and subsequent withdrawal of the agonists, see "Experimental Procedures"), CGS 21680 was no longer able to significantly increase cAMP levels (Fig. 4*B*). This demonstrates the existence of both homologous and D$_2$R-mediated heterologous desensitization of A$_{2A}$R. Instead, the inhibitory effect of quinpirole on forskolin-induced elevation of cAMP levels was about the same (40–50% inhibition) under basal conditions and after a 3-h incubation with the A$_{2A}$R or the D$_2$R agonist (Fig. 4, *A* and *B*). Thus, as already described, A$_{2A}$R clearly desensitized after A$_{2A}$R agonist incubation (18, 19) and D$_2$R (long form) showed resistance to D$_2$R agonist-induced desensitization (20). However, after 3 h of incubation with both quinpirole (50 μM) and CGS 21680 (200 nM), quinpirole (1 μM) inhibited forskolin-induced cAMP accumulation by only 17.1%/11.4% (median/interquartile range) (Fig. 4*C*). This effect, when compared with the effect of quinpirole on untreated cells, was significantly different (Mann-Whitney U test: $p < 0.01$). Hence, quinpirole was found to inhibit forskolin-induced cAMP accumulation by 40.7%/5.8% (median/interquartile range) (Fig. 4*C*). Therefore, costimulation of A$_{2A}$R and D$_2$R accelerates D$_2$R desensitization, likely by causing increased D$_2$R internalization (see above).

Coimmunoprecipitation of A$_{2A}$R and D$_2$R in Membrane Preparations from SH-SY5Y Neuroblastoma Cells and Ltk$^-$ Fibroblast Cells—The possible existence of A$_{2A}$R/D$_2$R heteromeric complexes was then analyzed by coimmunoprecipitation performed on membrane preparation of D$_2$R-transfected SH-SY5Y neuroblastoma cells. Immunoprecipitation with anti-A$_{2A}$R antibodies followed by Western blotting with anti-D$_2$R antibodies revealed three bands of 43, 47, and 63 kDa (Fig. 5), corresponding to different glycosylated states of the D$_2$R (21). The same three bands were also obtained in control lysate preparations (Fig. 5). On the other hand, immunoprecipitation with anti-A$_{2A}$R antibodies followed by Western blotting with anti-A$_1$R did not reveal any band corresponding to A$_1$R, indicating the absence of A$_{2A}$R-A$_1$R co-immunoprecipitation (Fig. 5). A Western blotting performed with control lysate preparations showed a band of ~40 kDa, which corresponds to the A$_1$R (Fig. 5). A$_{2A}$R/D$_2$R interactions were also examined in mouse fibroblast Ltk$^-$ cells stably transfected with the human D$_2$R (long form) or human D$_1$R (8, 9). These two cell lines express a similar density of transfected dopamine receptors (2.8 pmol/mg protein of D$_2$R in the D$_2$R-Ltk$^-$ cell line and 4.2 pmol/mg protein of the D1R in the D1R-Ltk$^-$ cell line (Refs. 8 and 9)). Both cell lines were transiently transfected with either dog A$_{2A}$R cDNA double-tagged with hemagglutinin (HA-A$_{2A}$R-HA) or an irrelevant plasmid. Antibodies against the hemagglutinin tag (anti-HA)

were able to precipitate a band of ~65 kDa detected in Western blot with the anti-D$_2$R antibodies but only from cells that express both D$_2$R and HA-A$_{2A}$R-HA (Fig. 6). This band corresponds to the highly glycosylated state of D$_2$R (21). As a positive control, we showed that this band could also be obtained from lysates of D$_2$R-transfected Ltk$^-$ cells, thus being independent of the presence of HA-A$_{2A}$R-HA. Antibodies against anti-HA failed to coimmunoprecipitate D$_1$R in cells expressing D$_1$R/HA-A$_{2A}$R antibodies, assessing for the specificity of the A$_{2A}$R/D$_2$R coimmunoprecipitation (Fig. 6). These results demonstrate for the first time that A$_{2A}$R and D$_2$R assemble into heteromeric complexes in two different cell lines that coexpress both receptors and that these complexes exist in the absence of exogenous agonists.

Colocalization and Coaggregation of A$_{2A}$R and D$_2$R in Cultured Striatal Neurons: Immunolabeling Experiments—A$_{2A}$R/D$_2$R interactions were also studied in neuronal primary cultures of rat striatum. Cells were grown for 2 weeks and immunostained for A$_{2A}$R and D$_2$R (see above). Immunolabeling of A$_1$R on nonpermeabilized cells was also performed. Most neurons exhibited A$_{2A}$R and D$_2$R IR in the soma and in the dendrites, however, with predominance of D$_2$R to A$_{2A}$R IR in the dendrites (Fig. 7*A*). As for neuroblastoma cells, confocal analysis revealed a high degree of A$_{2A}$R/D$_2$R colocalization in the absence of exposure to exogenous agonists (Fig. 7*A*). Treatment (6 h) with either the A$_{2A}$R agonist CGS 21680 (100 nM) or the D$_2$R agonist quinpirole (10 μM) induced aggregation of both A$_{2A}$R and D$_2$R (Fig. 7*A*) and reduction in IR intensity. However, no synergism was observed when cells were cotreated with CGS 21680 (100 nM) and quinpirole (10 μM) for the same time (Fig. 7*A*). To assess the specificity of A$_{2A}$R/D$_2$R interactions, cells were incubated with 10 μM quinpirole for 6 h and immunostained with anti-A$_1$R antibodies. No change in the pattern of distribution of A$_1$R present in the soma and dendrites was observed (Fig. 7*B*). In addition and instead of A$_{2A}$R/D$_2$R, no aggregates were seen, which confirms the specificity of A$_{2A}$R/D$_2$R interactions. Cointernalization experiments analogous to those described in Fig. 2 could not be performed in cultured striatal cells, which did not tolerate the temperature conditions of the experimental internalization protocol (cells changed morphology and fell off the coverslip).

Interaction between A$_{2A}$R and D$_2$R in Cultured Striatal Neurons: cAMP Accumulation Experiments—Both basal and forskolin-induced cAMP accumulation were about 10 times higher than in neuroblastoma cells (Fig. 8*A*). This could explain why, unlike what was observed in neuroblastoma cells, CGS 21680 (1 μM) did not induce any significant increase in cAMP accumulation compared with basal values (Fig. 8*A*). As for neuroblastoma cells, quinpirole (1 μM) did not modify cAMP levels
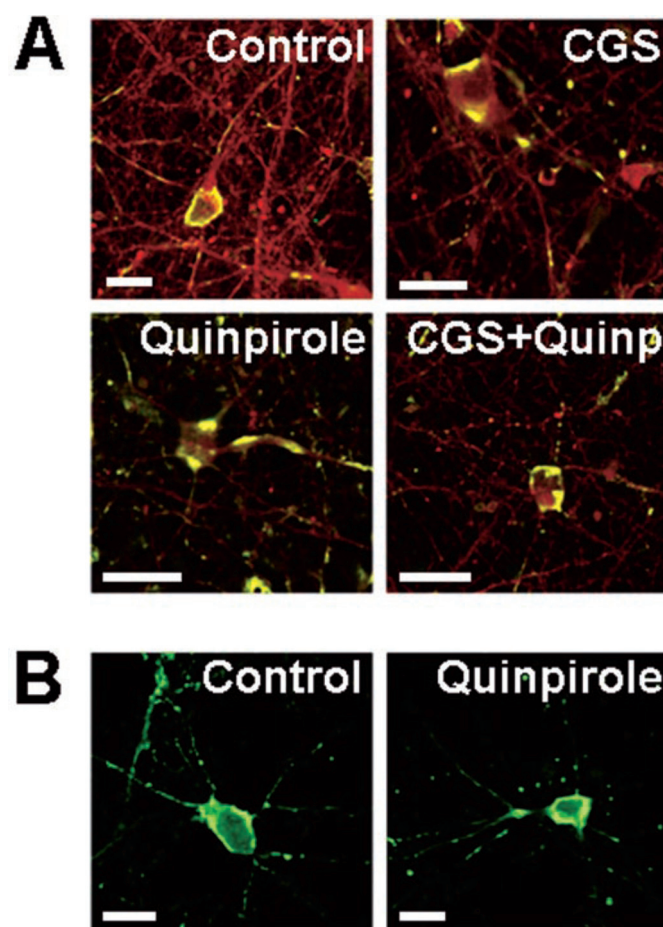
FIG. 7. **Double immunofluorescence staining and confocal images of striatal neurons in culture.** *Panel A*, cells were exposed for 6 h to either 100 nM CGS-21680, 10 μM quinpirole, or both and were processed for immunostaining using fluorescein (*green*)-conjugated rabbit anti-A$_{2A}$R antibodies and rhodamine (*red*)-conjugated rabbit anti-D$_2$R antibodies. The cells were analyzed by confocal microscopy. Superimposition of images reveals the colocalization of A$_{2A}$R and D$_2$R in *yellow*. *Panel B*, staining of adenosine A$_1$R with fluorescein (*green*)-conjugated anti-A$_1$R antibodies. Note the lack of effect of 10 μM quinpirole (6 h). Representative images from four to five independent experiments/treatment are shown; *scale bar*, 10 μm.
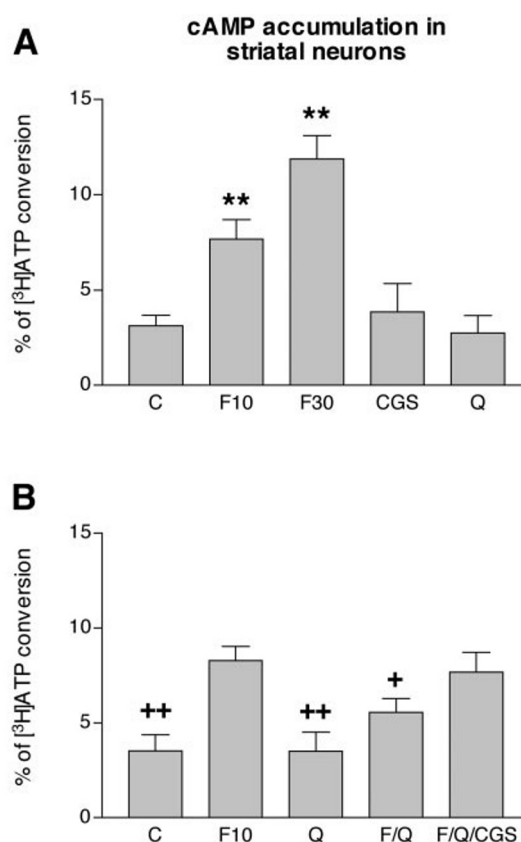

FIG. 8. **cAMP accumulation experiments in striatal neurons in culture.** Results represent means $\pm$ S.E. and are expressed as percentage of conversion of total [^{3}H]ATP to [^{3}H]cAMP ($n = 10$–14). *A*, effects of 10 and 30 μM forskolin (*F10* and *F30*, respectively), 1 μM CGS 21680 (*CGS*), and 1 μM quinpirole (*Q*). Forskolin, but not CGS 21680, significantly increased cAMP accumulation. **, $p < 0.01$ compared with control (*C*); one-way ANOVA. *B*, effects of 10 μM forskolin (*F*), 1 μM CGS 21680 (*CGS*), and 1 μM quinpirole (*Q*), alone or in combination. CGS 21680 counteracted the inhibitory effect of quinpirole on forskolin-induced cAMP accumulation. + and ++, $p < 0.05$ and $p < 0.01$, respectively, compared with forskolin; one-way ANOVA and *post hoc* Scheffe's multiple comparison test.

but significantly reduced forskolin (10 μM)-induced cAMP accumulation (Fig. 8*B*). Finally, CGS 21680 (1 μM) counteracted the effect of quinpirole on forskolin-induced cAMP accumulation (Fig. 8*B*). These results provide a functional demonstration of the antagonistic A$_{2A}$R/D$_2$R interactions in striatal neurons in culture.

DISCUSSION

The main findings of the present work are first that A$_{2A}$R and D$_2$R are colocalized and form heteromers in untreated neuronal cells and that they coaggregate upon long term exposure to either agonist. The formation of A$_{2A}$R/D$_2$R heteromers and aggregates is receptor subtype-specific because co-expression of A$_{2A}$R/D$_1$R (present study) or A$_1$R/D$_2$R (6) does not lead to formation of heteromers. Furthermore, A$_{2A}$R did not form heteromeric complexes with A$_1$R (present study). This phenomenon may therefore constitute the molecular basis for the selective A$_{2A}$R/D$_2$R interactions observed *in vitro*, like A$_{2A}$R modulation of D$_2$ binding characteristics (7, 8, 22, 23), counteraction of D$_2$R-mediated intracellular [Ca^{2+}i] responses (7), and inhibition of cAMP accumulation (see Ref. 23 and present paper). The same type of antagonism was observed *in vivo* with the A$_{2A}$R inhibition of D$_2$R-mediated regulation of GABA release in the globus pallidus and of D$_2$R-mediated

increases in motor activity (1, 5). Besides acute antagonistic actions, the A$_{2A}$R/D$_2$R heteromers may be involved in receptor trafficking, because long term exposure to either A$_{2A}$R or D$_2$R agonists induces aggregation and cotreatment with these agonists induces internalization of both receptors. Moreover, prior exposure to A$_{2A}$R or D$_2$R agonists can produce a desensitization of the A$_{2A}$R in terms of cAMP accumulation associated with coaggregation. In contrast, co-exposure to A$_{2A}$R and D$_2$R agonists, but not to any of the two agonists alone, causes desensitization of D$_2$R-mediated inhibition of cAMP accumulation, which is associated with cointernalization. The present observation that A$_{2A}$R and D$_2$R functions are simultaneously altered after long exposure to agonists can aid in understanding behavioral findings involving cross-tolerance and cross-sensitization between dopamine agonists and compounds active at adenosine receptors (such as caffeine) (24, 25). Together with other recently reported findings, the present results suggest that changes in A$_{2A}$R function may be involved in the secondary effects observed after chronic intermittent treatment with L-DOPA such as reduced antiparkinsonian activity and dyskinesia (26). Adenosine is a feedback detector of neuronal activation, in view of the fact that it allows the neuronal network to return into a resting state (27). Adenosine is therefore expected to increase in the striatal extracellular fluid from patients with Parkinson's disease mainly after chronic intermittent L-DOPA

treatment and in agreement with the evidence of increased striatal glutamate drive (28). Hence, striatal extracellular levels of adenosine have been found to increase in the 1-methyl-4-phenyl-1,2,3,6-tetrahydropyridine model of Parkinson's disease (29). Thus, the wearing off of the antiparkinsonian action of L-DOPA treatment may in part be caused by the simultaneous chronic activation of A$_{2A}$R and D$_2$R that, according to the present results, may lead to substantial cointernalization of both receptors. The coadministration of A$_{2A}$R antagonists together with L-DOPA or dopamine D$_2$R agonists may therefore provide a new therapeutic approach lacking the secondary effects of chronic L-DOPA treatment (30, 31). Overall, the present and previous (1, 5) data implicate that the membrane interactions taking place between A$_{2A}$R and D$_2$R via heteromeric complexes represent a crucial mechanism influencing D$_2$R-mediated transmission. This prompts development of adenosine and dopamine antagonists/agonists compounds preferentially active on A$_{2A}$R/D$_2$R heteromers as new drugs for the treatment of neuropsychiatric diseases, such as Parkinson's disease (30, 31), schizophrenia (32, 33), Huntington's disease (34), and dystonia (35), in which D$_2$R have been implicated.

REFERENCES

1. Ferré, S., Fredholm, B. B., Morelli, M., Popoli, P., and Fuxe, K. (1997) *Trends Neurosci.* **20,** 482–487
2. Schiffmann, S. N., Jacobs, O., and Vanderhaeghen, J.-J. (1991) *J. Neurochem.* **57,** 1062–1067
3. Fink, J. S., Weaver, D. R., Rivkees, S. A, Peterfreund, R. A., Pollack, A. E., Adler, E. M., and Reppert, S. M. (1992) *Mol. Brain Res.* **14,** 186–195
4. Ferré, S., O'Connor, W. T., Svenningsson, P., Bjorklund, L., Lindberg, J., Tinner, B., Stromberg, I., Goldstein, M., Ogren, S. O., Ungerstedt, U., Fredholm, B. B., and Fuxe, K. (1996) *Eur. J. Neurosci.* **8,** 1545–1553
5. Fuxe, K., Ferré, S., Zoli, M., and Agnati, L. F. (1998) *Brain Res. Rev.* **26,** 258–273
6. Ginés, S., Hillion, J., Torvinen, M., Le Crom, S., Casado, V., Canela, E. I., Rondin, S., Lew, J. Y., Watson, S., Zoli, M., Agnati, L. F., Vernier, P., Lluis, C., Ferré, S., Fuxe, K., and Franco, R. (2000) *Proc. Natl. Acad. Sci. U. S. A.* **97,** 8606–8611
7. Salim, H., Ferré, S., Dalal, A., Peterfreund, R. A., Fuxe, K., Vincent, J. D., and Lledo, P. M. (2000) *J. Neurochem.* **74,** 432–439
8. Dasgupta, S., Ferré, S., Kull, B., Hedlund, P. B., Finnman, U. B., Ahlberg, S., Arenas, E., Fredholm, B. B., and Fuxe, K. (1996) *Eur. J. Pharmacol.* **316,** 325–331
9. Ferré, S., Torvinen, M., Antoniou, K., Irenius, E., Civelli, O., Arenas, E., Fredholm, B. B., and Fuxe, K. (1998) *J. Biol. Chem.* **273,** 4718–4724
10. Sarrio, S., Casado, V., Escriche, M., Ciruela, F., Mallol, J., Canela, E. I., Lluis, C., and Franco, R. (2000) *Mol. Cell. Biol.* **20,** 5164–5174
11. Bjelke, B., Goldstein, M., Tinner, B., Andersson, C., Sesack, S. R., Steinbusch, H. W., Lew, J. Y., He, X., Watson, S., Tengroth, B., and Fuxe, K. (1996) *J. Chem. Neuroanat.* **12,** 37–50
12. Saura, C. A., Mallol, J., Canela, E. I., Lluis, C., and Franco, R. (1998) *J. Biol. Chem.* **273,** 17610–17617
13. Ciruela, F., Casado, V., Mallol, J., Canela, E. I., Lluis, C., and Franco, R. (1995) *J. Neurosci. Res.* **42,** 818–828
14. Duncan, O. D. (1977) in *The Measurement of Population* (Smith, D., and Keyfitz, N., eds) pp. 349–363, Springer Verlag, London
15. Agnati, L. F., Fuxe, K., Zini, I., Calza, L., Benfenati, F., Zoli, M., Hokfelt, T., and Goldstein, M. (1982) *Neurosci. Lett.* **32,** 253–258
16. Olah, M. E. (1997) *J. Biol. Chem.* **272,** 337–344
17. Salomon, Y., Londos, C., and Rodbell, M. (1974) *Anal. Biochem.* **58,** 541–548
18. Palmer, T. M., Gettys, T. W., Jacobson, K. A., and Stiles, G. L. (1994) *Mol. Pharmacol.* **45,** 1082–1094
19. Mundell, S. J., and Kelly, E. (1998) *Br. J. Pharmacol.* **125,** 1594–1600
20. Ng, G. Y., Varghese, G., Chung, H. T., Trogadis, J., Seeman, P., O'Dowd, B. F., George, S. R. (1997) *Endocrinology* **138,** 4199–4206
21. Fishburn, C. S., Elazar, Z., and Fuchs, S. (1995) *J. Biol. Chem.* **270,** 29819–29824
22. Ferré, S., von Euler, G., Johansson, B., Fredholm, B. B., and Fuxe, K. (1991) *Proc. Natl. Acad. Sci. U. S. A.* **88,** 7238–7241
23. Kull, B., Ferré, S., Arslan, G., Svenningsson, P., Fuxe, K., Owman, C., and Fredholm, B. B. (1999) *Biochem. Pharmacol.* **58,** 1035–1045
24. Fenu, S., Cauli, O., and Morelli, M. (2000) *Behav. Brain. Res.* **114,** 97–105
25. Garrett, B. E., and Holtzman, S. G. (1994) *Eur. J. Pharmacol.* **262,** 65–75
26. Zeng, B. Y., Pearce, R. K., MacKenzie, G. M., and Jenner, P. (2000) *Eur. J. Neurosci.* **12,** 1096–1104
27. Ferré, S., and Fuxe, K. (2000) *Prog. Brain Res.* **125,** 353–361
28. Chase, T. N., and Oh J. D. (2000) *Trends Neurosci.* **23,** S86–S91
29. Nomoto, N., Kaseda, S., Iwata, S., Shimizu, T., Fukuda, T., and Nakagawa, S. (2000) *J. Neurol.* **247,** V16-V22
30. Kanda, T., Jackson, M. J., Smith, L. A., Pearce, R. K., Nakamura, J., Kase, H., Kuwana, Y., and Jenner, P. (1998) *Ann. Neurol.* **43,** 507–513
31. Stromberg, I., Popoli, P., Muller, C. E., Ferré, S., and Fuxe, K. (2000) *Eur. J. Neurosci.* **12,** 4033–4037
32. Ferré, S. (1997) *Psychopharmacology* **133,** 107–120
33. Akhondzadeh, S., Shasavand, E., Jamilian, H., Shabestari, O., and Kamalipour, A. (2000) *J. Clin. Pharmacol. Ther.* **25,** 131–137
34. Popoli, P., Pezzola, A., Reggio, R., Caporali, M. G., and Scotti de Carolis, A. (1994) *Eur. J. Pharmacol.* **257,** R5–R6
35. Richter, A., Hamann, M., and Bartling, C. (2000) *Eur. J. Pharmacol.* **404,** 299–302.(2000)